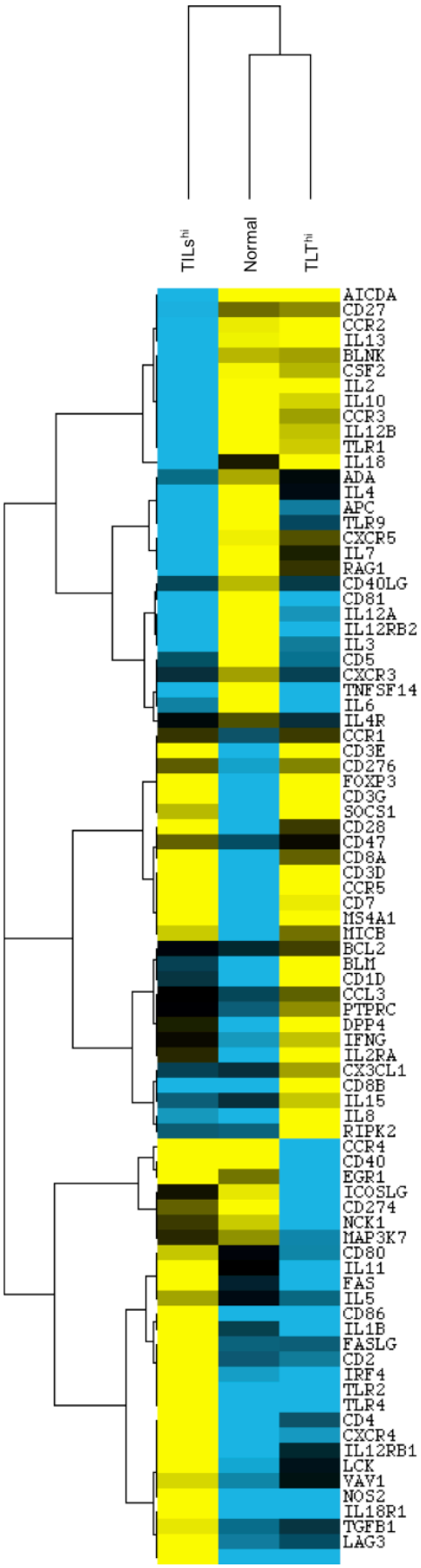

Figure S1. **Immune signature of human PDAC specimens with different patterns of B cell distribution.** Heatmap showing gene expression analysis of RNA extracted from paraffin embedded tissue specimens of human PDAC, categorized as TLT^{hi} (n=3) or $TILs^{hi}$ (n=3) after immunohistochemical evaluation with an anti CD20 antibody, and from normal pancreata (n=3) as a control. Sample clustering follows the pattern of B cell distribution (i.e. TLT^{hi} and $TILs^{hi}$ samples segregating together), suggesting that B cell distribution identifies specific gene expression programs. In the dendrogram, the height of vertical lines reflects the distance between the pair of clusters.

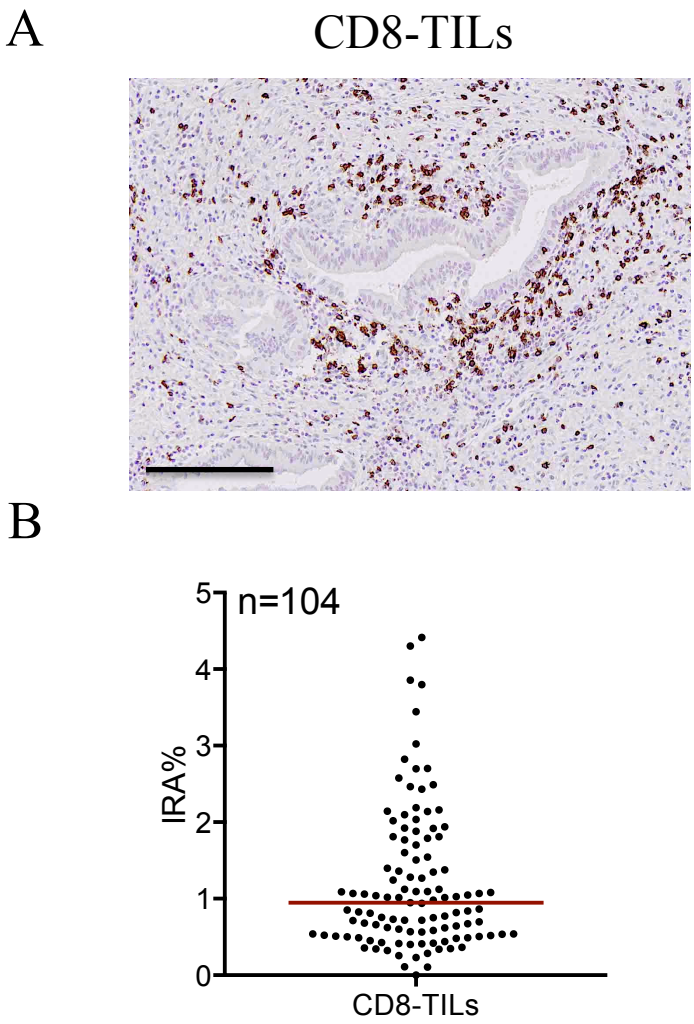

Figure S2. **CD8 T cells in human PDAC.** (**A**) Histological section of human PDAC, stained with an anti-CD8 antibody evidences CD8-TILs at the tumor-stroma interface. (**B**) Distribution of CD8-TIL IRA% across 104 PDAC patients. Bar: 200 μm.

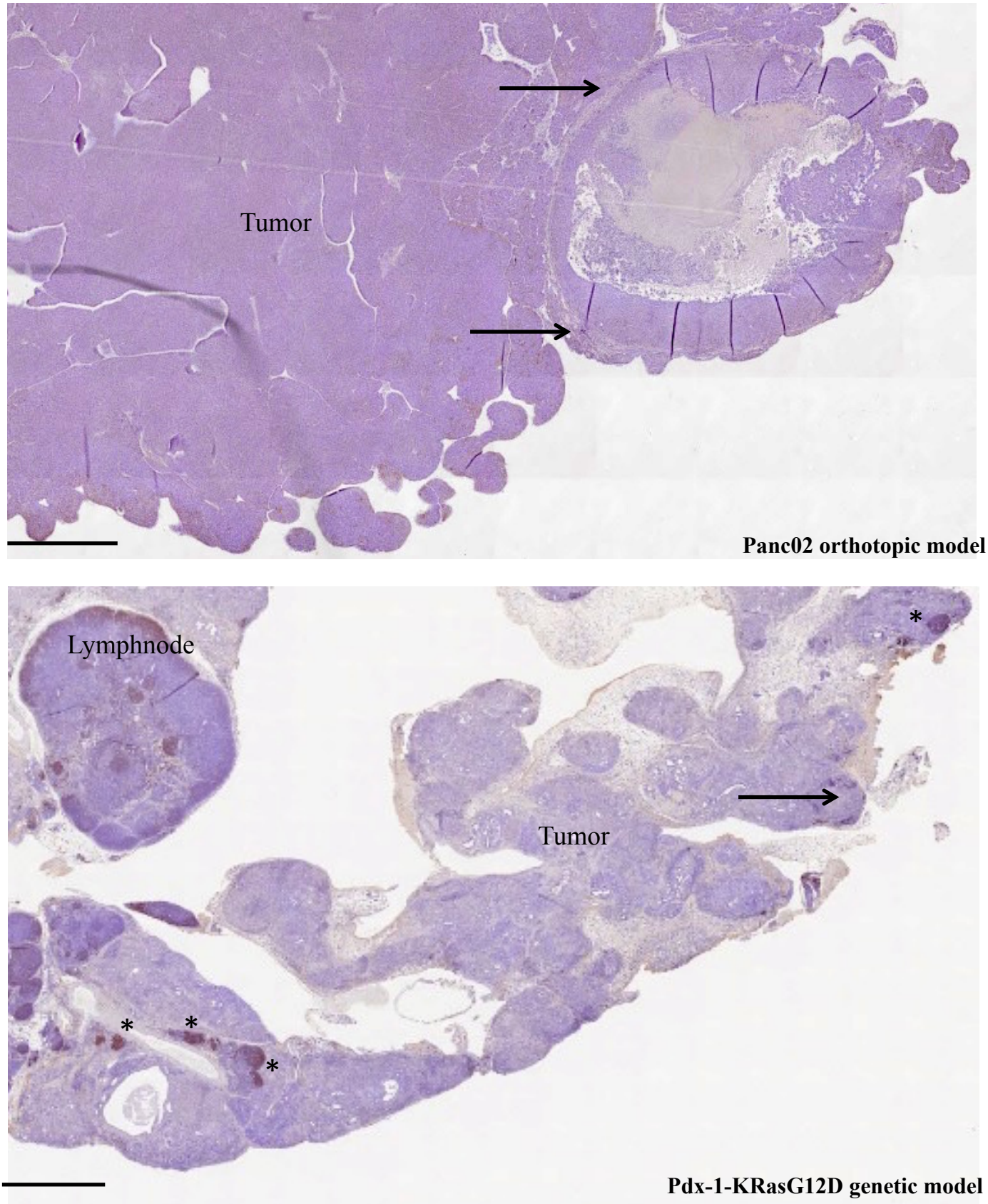

Figure S3. **TLT occurrence in implanted versus genetic PDAC models.** Representative whole slide scans of sections stained with an anti-B220 antibody, from mice orthotopically implanted with PDAC cells (upper panel) and Pdx1-KRasG12D mice spontaneously developing PDAC (lower panel). Arrows indicate B220-TILs, asterisks indicate B220-TLT (scale bars: 1 mm).

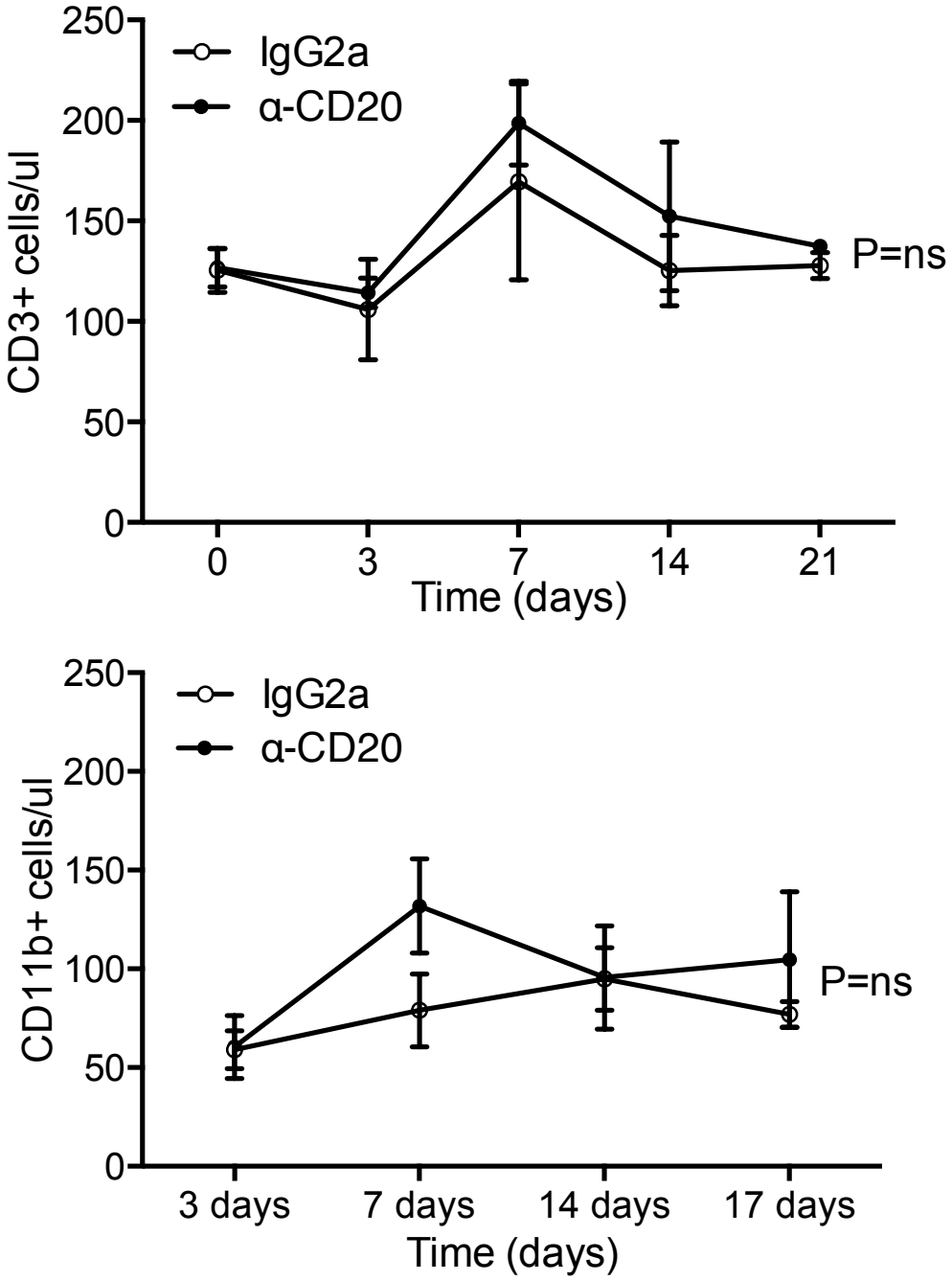

Figure S4. **Blood cell counts after α-CD20 treatment.** $CD3^+$ T cells (upper panel) and $CD11b^+$ myeloid cells (lower panel) blood cell counts in IgG2A (n=3) and α-CD20 treated (n=3) mice, at different time points. P value by Students' t test.

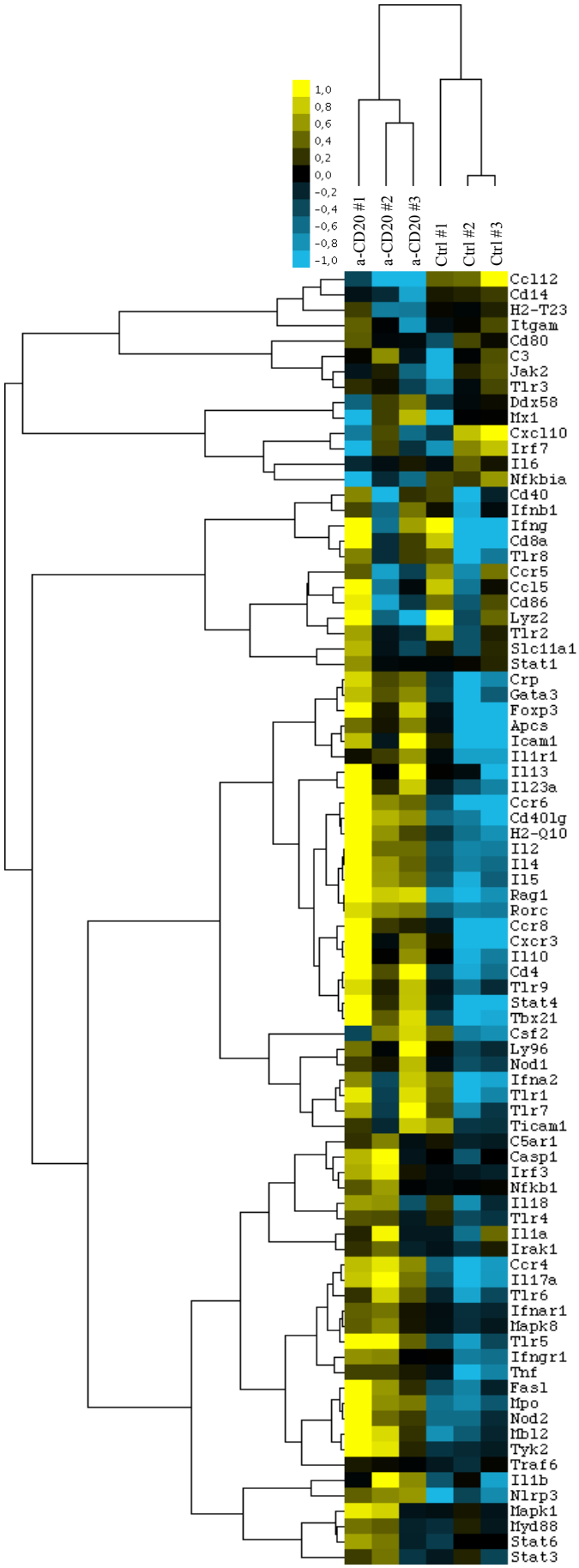

Figure S5. **Immune signature of leukocytes from PDAC tumors after α-CD20 treatment.** Heatmap showing the immune signature of the leukocyte population isolated from PDAC tumors from control and α-CD20 treated mice. Height of vertical lines in the dendrogram reflects the distance between the pair of clusters.

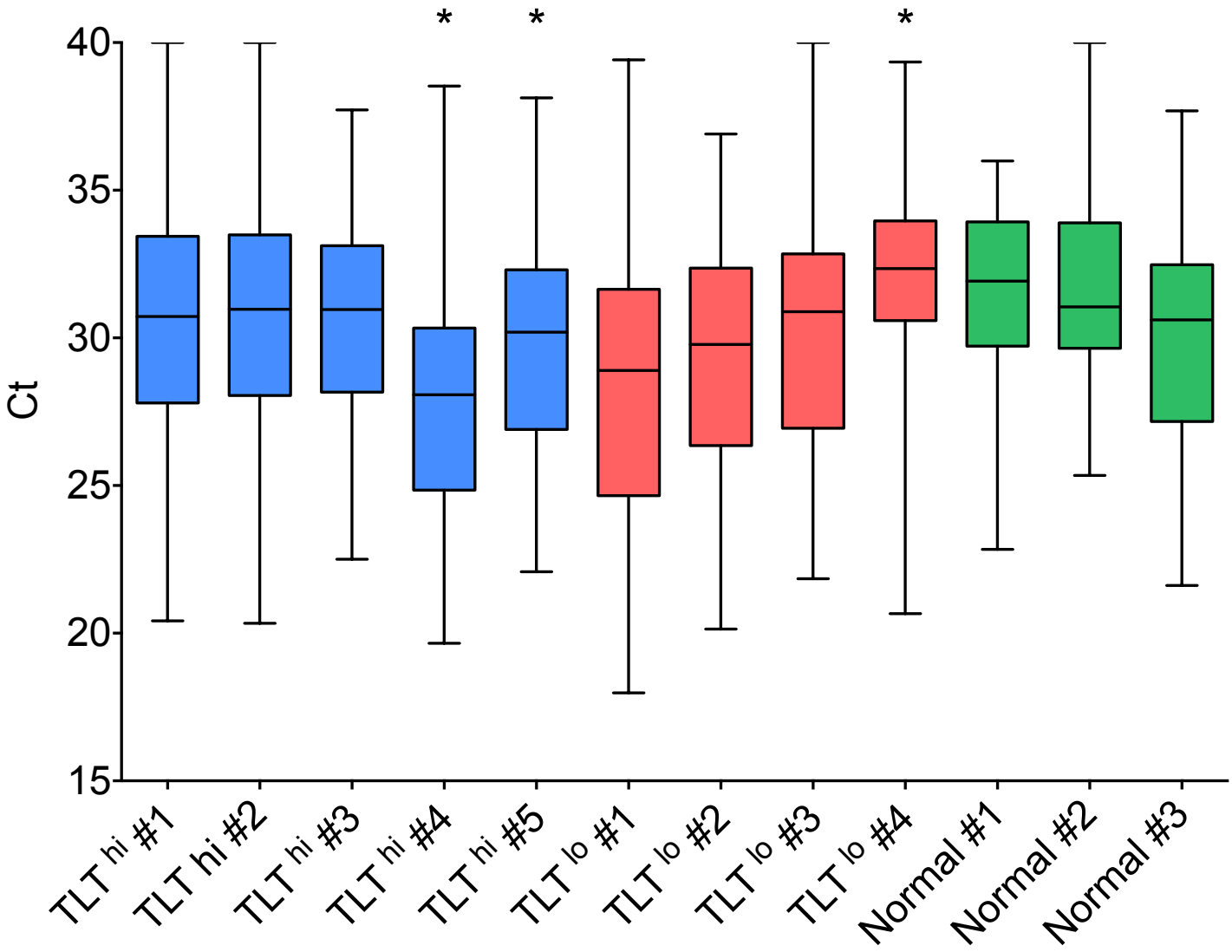

Figure S6. **Quality check of RNA from paraffin-embedded tissue specimens.** Within a specific group (TLThi, TLTlo), samples with the lowest Ct variability (n=3) were selected for further gene expression analysis. ∗ indicates removed samples.

Table S1. Densities of CD20-TLT, CD20-TILs and CD8-TILs in 104 pancreatic ductal adenocarcinoma.

				CD20-TLT [a, b]		CD20-TILs[a, b]		CD8-TILs[a, b]	
		n	(%)	median	P	median	P	median	P
All cases		104	(100)	3.72		0.41		0.61	
Patient demographics									
Age (years)[c]		104	(100)	-	0,170	-	0.086	-	0.432
Gender	Female	54	(51.9)	3.90	Ref	0.38	Ref	0,61	Ref
	Male	50	(48.1)	3.35	0.464	0.44	0.686	0.60	0.502
Tumor features									
Nodal involvement	No	35	(33.6)	3.14	Ref	0,38	Ref	0,44	Ref
	Yes	67	(64.4)	4.31	0.857	0.45	0.325	0.64	0.187
Local Invasion	pT1-pT2	11	(10.6)	3.68	Ref	0,32	Ref	0,41	Ref
	pT3-pT4	91	(87.5)	4.02	0.431	0,43	0.456	0.61	0.375
Grade [d]	G1/ G2	47	(45.2)	4.17	Ref	0.38	Ref	0.57	Ref
	G3/ G4	44	(42.3)	3.53	0.351	0.47	0.816	0.64	0.930
Chemotherapy (CTX)									
Adjuvant	No	35	(33.7)	3.83	Ref	0.36	Ref	0.64	Ref
	Yes	69	(66.3)	3.56	0.937	0.43	0.575	0.57	0.310
Neo-Adjuvant	No	90	(86.5)	4.02	Ref	0.41	Ref	0.63	Ref
	Yes	14	(13.5)	2.01	0.200	0.42	0.848	0.39	0.287

[a] Density is expressed as percent immunoreactive area (IRA%) at the tumor-stroma interface.
[b] Linear regression analysis; CD20-TLT, CD20-TIL and CD8-TIL densities were entered as dependent continuous variables.
[c] Age was entered as independent continuous variable.
[d] G1/G2, well-to moderately differentiated; G3/G4, poorly differentiated.